Available online at www.sciencedirect.com
ScienceDirect
Journal of Molecular Catalysis A: Chemical 261 (2007) 147–155
JOURNAL OF MOLECULAR CATALYSIS A: CHEMICAL
www.elsevier.com/locate/molcata

Oxidation of cyclohexene with *tert*-butylhydroperoxide catalysted by host (nanocavity of zeolite-Y)/guest (Mn(II), Co(II), Ni(II) and Cu(II) complexes of *N*,*N*′-bis(salicylidene)phenylene-1,3-diamine) nanocomposite materials (HGNM)

Masoud Salavati-Niasari [a,*], Maryam Shaterian [b], Mohammad Reza Ganjali [c], Parviz Norouzi [c]

[a] *Institute of Nano Science and Nano Technology, University of Kashan, Kashan, P.O. Box. 87317-51167, Iran*
[b] *Department of Chemistry, University of Kashan, Kashan, P.O. Box. 87317-51167, Iran*
[c] *Center of Excellence in Electrochemistry, Department of Chemisrtry, Tehran University, Tehran, Iran*

Received 18 March 2006; received in revised form 18 July 2006; accepted 18 July 2006
Available online 8 September 2006

Abstract

Transition metal (M = Mn(II), Co(II), Ni(II) and Cu(II)) complexes with tetradendate Schiff-base ligand; *N*,*N*′-bis(salicylidene)phenylene-1,3-diamine, H_2[sal-1,3-phen]; was entrapped in the nanocavity of zeolite-Y by a two-step process in the liquid phase: (i) adsorption of bis(salicylaldiminato)metal(II); [M(sal)$_2$]-NaY; in the supercages of the zeolite, and (ii) in situ Schiff condensation of the metal(II) precursor complex with the corresponding phenylene-1,3-diamine; [M(sal-1,3-phen)]-NaY. The new materials were characterised by several techniques: chemical analysis, spectroscopic methods (DRS, BET, FTIR and UV–vis), conductometric and magnetic measurements. Analysis of the data indicates that the M(II) complexes are encapsulated in the nanodimensional pores of zeolite-Y and exhibit different from those of the free complexes, which can arise from distortions caused by steric effects due to the presence of sodium cations, or from interactions with the zeolite matrix. The host–guest nanocomposite materials (HGNM); [M(sal-1,3-phen)]-NaY; catalyzes the oxidation of cyclohexene with *tert*-butylhydroperoxide (TBHP). Oxidation of cyclohexene with [M(sal-1,3-phen)] gave 2-cyclohexene-1-one, 2-cyclohexene-1-ol and 1-(*tert*-butylperoxy)-2-cyclohexene whereas, oxidation with [M(sal-1,3-phen)]-NaY resulted in the formation of 2-cyclohexene-1-one and 2-cyclohexene-1-ol. [Mn(sal-1,3-phen)]-NaY shows significantly higher catalytic activity than other catalysts.

Keywords: Schiff-base; Zeolite; Oxidation; Cyclohexene; Host–guest nanocomposite

1. Introduction

Nanocavity of zeolite encapsulation of transition metal complexes with redox catalytic activity is a theme of current research [1–5] due to their potential use as heterogeneous redox catalysts. The heterogenisation process constrains the metal complexes within the support, due to spatial restrictions, Coulombic interactions or covalent bonding. The complexes are expected to retain their catalytic homogeneous properties or to have them synergistically enhanced by the properties of the zeolites, shape selectivity, electrostatic potential and acidic properties. Besides their main application as heterogeneous catalysts, these hybrid systems provide information, at the molecular level, on the interactions between the host (nanocavity of zeolite) and their guest (complexes). A substantial number of articles have been published on the preparation and characterisation of metal complex such as [M(salen)] modified zeolites, with special emphasis on the structural and electronic properties of the complexes in the zeolite micro-environment [1–5]. Due to the complexity of these systems, some aspects of the host–guest interactions are still obscure, and not all questions regarding these interactions have been adequately addressed.

We have synthesised several complexes of transition metal with polydentate ligands, and have studied their electronic, struc-

* Corresponding author. Tel.: +98 361 555 5333; fax: +98 361 555 2930.
E-mail address: salavati@kashanu.ac.ir (M. Salavati-Niasari).

1381-1169/$ – see front matter © 2006 Elsevier B.V. All rights reserved.
doi:10.1016/j.molcata.2006.07.048

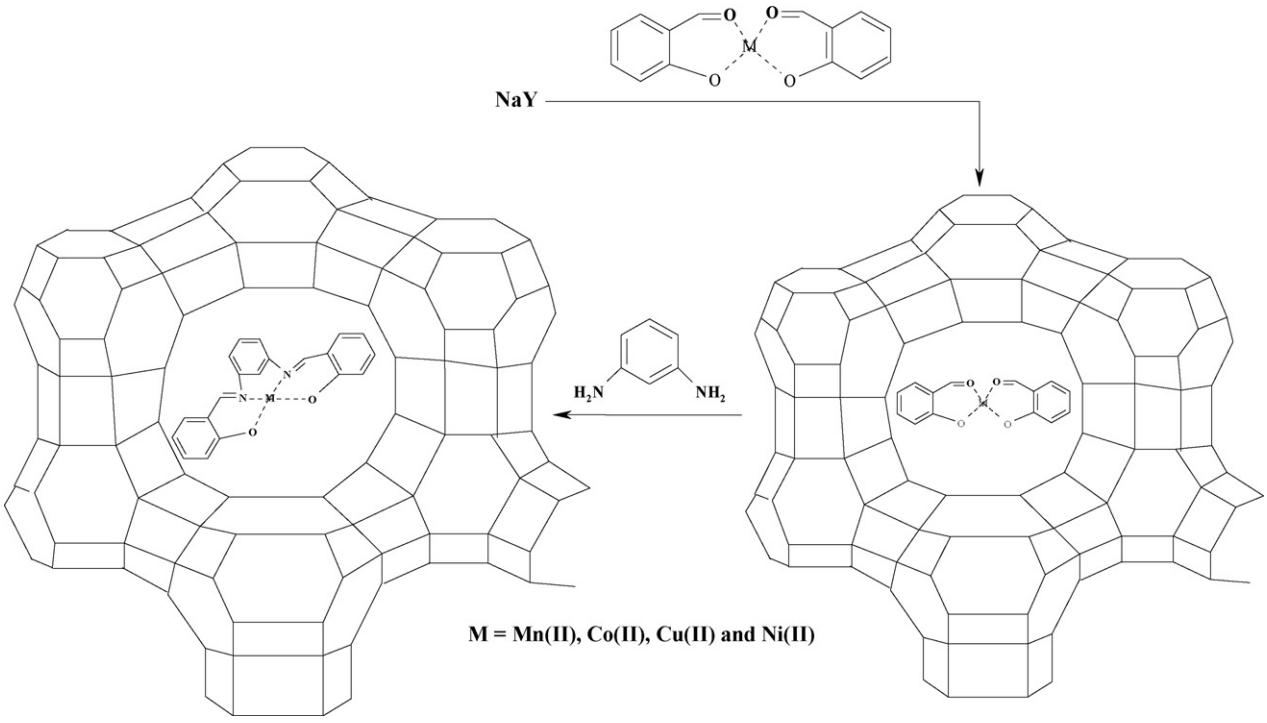

Scheme 1.

tural and redox properties in solution [6–10]. Presently, we are extending our studies to the encapsulation of these metal complexes in zeolites, and to assess the effect of encapsulation on the physical–chemical properties of the complexes relative to those in solution, with the ultimate aim of studying their catalytic behavior in the activation of molecules.

Several approaches have been used for the encapsulation of transition metal complexes in zeolite supercages [1–10]; the choice of any specific method is dictated by the size of the ligand relative to the free diameter of the zeolite channels. Complexes or ligands that are smaller than the channels can be adsorbed from a solution phase into the zeolite, or they can be synthesised via diffusion of the ligand into a metal-exchanged zeolite (flexible ligand method, FLM). For complexes or ligands that are larger than the diameters of the channels, two approaches to prepare zeolites with encapsulated complexes have been developed. In one, the ligand is synthesised in situ in the presence of the transition metal ion, that can exist in the reaction media as a precursor complex, or that is exchanged into the zeolite. In the other, the pre-formed complexes are used as templates during zeolite synthesis (template synthesis method, TSM).

In this work, we report the encapsulation of transition metal complexes (Scheme 1) in the supercages of a NaY zeolite, using the same sequential procedure: (i) diffusion of $[M(sal)_2]$, and (ii) in situ Schiff condensation with the phenylene-1,3-diamine. The use of a zeolite with the FAU topology, such as NaY zeolite, may circumvent hydrolysis of the occluded complexes. We will also address the effect on the structural and electronic properties of the encapsulated complexes within a host with: (i) a negative charge which can hence act as a stronger ligand, and (ii) a larger number of charge-compensating cations thus providing less free space within the zeolite cavities.

2. Experimental

2.1. Materials and physical measurements

All the solvents were purchased from Merck (pro analysi) and were distilled and dried using molecular sieves (Linda 4 Å). Manganese(II), copper(II), nickel(II) and cobalt(II) acetate, salicylaldehyde, phenylene-1,3-diamine and *tert*-butylhydroperoxide (solution 80% in di-*tert*-butylperoxide) were obtained from Merck Co. Cyclohexene was distilled under nitrogen and stored over molecular sieves (4 Å). The precursor complexes; bis(salicylaldiminato)metal(II); were prepared according to the procedure described previously [11]. Cyclohexanone was used as an internal standard for the quantitative analysis of the product using gas chromatography. Reference samples of cyclohexene oxide, 2-cyclohexene-1-ol and 2-cyclohexene-1-one (Aldrich) were distilled and stored in the refrigerator. NaY with the Si:Al ratio of 2.53 was purchased from Aldrich (Lot No. 67812). XRD patterns were recorded by a Rigaku D-max C III, X-ray diffractometer using Ni-filtered Cu Kα radiation. Elemental analyses were obtained from Carlo ERBA Model EA 1108 analyzer.

The metal contents of the samples were measured by atomic absorption spectrophotometer (AAS-Perkin-Elmer 4100–1319) using a flame approach. After completely destroying the zeolitic framework with hot and concentrated HCl, sodium, aluminum and nickel were analyzed by AAS and SiO_2 was determined by gravimetric analysis. The products were analyzed by GC-MS, using a Philips Pu 4400 Chromatograph (capillary column: DB5MS, 30 m), Varian 3400 Chromatograph (15 m capillary column of HP-5; FID) coupled with a QP Finnegan MAT INCOF 50, 70 eV. Diffuse reflectance spectra (DRS) were regis-

Table 1
Elemental analysis, vibrations parameters and some physical properties for Schiff-base neat metal(II) complexes

Com plex	Found (calculated)					Λ_M[a] (Ω^{-1} cm^2 M^{-1})	μ_{eff} (MB)	IR (KBr, cm^{-1})			d↔d (nm)[b]
	%C	%H	%N	C/N	%M			υ(C=N)	υ(C–O)	υ(C=C) Ring	
H_2(sal-1,3-phen)	75.78 (75.93)	4.94 (5.09)	8.97 (8.85)	8.45 (8.58)				1615	1276	1587 1510, 1450	
[Mn(sal-1,3-phen)]	64.89 (65.05)	3.70 (3.82)	7.69 (7.58)	8.44 (8.58)	14.72 (14.88)	18	5.93	1626	1283	1596 1540, 1495	
[Co(sal-1,3-phen)]	64.22 (64.35)	3.69 (3.78)	7.61 (7.50)	8.44 (8.58)	15.64 (15.79)	16	1.73	1620	1230	1584 1525, 1469	425
[Ni(sal-1,3-phen)]	64.28 (64.40)	3.66 (3.78)	7.67 (7.51)	8.38 (8.58)	15.60 (15.73)	10	−0.005	1610	1200	1576 1520, 1465	479
[Cu(sal-1,3-phen)]	63.43 (63.57)	3.68 (3.73)	7.53 (7.41)	8.42 (8.58)	16.69 (16.82)	12	1.74	1608	1339	1578 1521, 1460	490,560

[a] In DMSO solution.
[b] In chloroform solutions.

tered on a Shimadzu UV/3101 PC spectrophotometer the range 1500–200 nm, using MgO as reference. The stability of the supported catalyst was checked after the reaction by UV–vis and possible leaching of the complex was investigated by UV–vis in the reaction solution after filtration of the encapsulated zeolite. Nitrogen adsorption measurements were performed at 77 K using a Coulter Omnisorb 100CX instrument. The samples were degassed at 150 °C until a vacuum better than 10^{-3} Pa was obtained. Micropore volumes were determined by the *t*-method; a "monolayer equivalent area" was calculated from the micropore volume [12].

2.2. Preparation of *N,N′-bis(salicylidene) phenylene-1,3-diamine; H_2[sal-1,3-phen]*

The stoichiometric amount of salicylaldehyde (0.02 mol, 2.44 g) in dissolved methanol (25 ml) is added drop by drop to phenylene-1,3-diamine solution (0.01 mol, 1.08 g) in 25 ml methanol). The contents were refluxed for 3 h and a yellow precipitate of symmetrical Schiff-base ligand; (H_2[sal-1,3-phen]; was obtained. The yellow precipitate was separated by filtration, washed and dried in vacuum. It was then recrystallized from methanol to yield 86%. Elemental and spectroscopic analysis of neat and zeolite-encapsulated complexes confirmed the molecular composition of ligand (Tables 1 and 2).

2.3. Preparation of *[M(sal-1,3-phen)]*

The flask containing a stirred suspension of transition metal(II) acetate tetrahydrate (0.016 mol) in 100 ml propanol (was purged with nitrogen), and then warmed to 50 °C under a nitrogen atmosphere. *N,N′*-bis(Salicylidene)-1,3-phenylenediamine; H_2[sal-1,3-phen]; (5.06 g, 0.016 mol) and NEt_3 (4.46 ml, 0.032 mmol) were added in one portion, and the resulting suspension was then stirred and heated under reflux under a nitrogen atmosphere for 8 h. Then the mixture was cooled and filtered under reduced pressure. The collected solid was washed with diethylether and dried in air to give coloured crystalline [M(sal-1,3-phen)] which was purified by recrystallization from chloroform.

2.4. Preparation of *[M(sal)$_2$]-NaY*

Typically a 4 g sample of NaY zeolite was mixed with 0.36 g of bis(salicylaldiminato)metal(II) (which corresponds to about 50% supercage loading), suspended in 40 ml of $CHCl_3$ and then refluxed for 8 h. The coloured solid consisting of [M(sal)$_2$] entrapped in NaY and denoted as [M(sal)$_2$]-NaY was collected by filtration, washed with cold ethanol (10 ml) and then dried at 90 °C under vacuum for 5 h.

2.5. Preparation of *[M(sal-1,3-phen)]-NaY*

Two grams of [M(sal)$_2$]-NaY was refluxed with a three-fold excess of phenylene-1,3-diamine in CH_3Cl. After a 3-h reflux, the solid samples, [M(sal-1,3-phen)]-NaY, were filtered

Table 2
Chemical composition, DRS absorption, Surface area, pore volume data and IR stretching frequencies (as KBr pellets) of zeolite-encapsulated manganese(III) complexes

Sample	C (%)	H (%)	N (%)	C/N	Si (%)	Al (%)	Na (%)	M (%)	Si/Al	$\upsilon_{C=N}$ (cm^{-1})	d ↔ d (cm^{-1})	Surface area (m^2/g)[a]	Pore volume (ml/g)[b]
NaY	–	–	–	–	21.76	8.60	7.50		2.53	–	–	545	0.31
Mn(II)-NaY	–	–	–	–	22.08	8.73	3.34	2.58	2.53	–	–	535	0.30
[Mn(sal-1,3-phen)-NaY]	3.46	1.28	0.42	8.16	21.68	8.57	5.34	2.30	2.53	1624	–	410	0.26
Co(II)-NaY	–	–	–	–	21.53	8.53	3.36	3.71	2.53	–	–	532	0.30
[Co(sal-1,3-phen)-NaY]	3.41	1.27	0.42	8.21	21.20	8.38	5.30	2.28	2.53	1616	423	396	0.23
Ni(II)-NaY	–	–	–	–	21.79	8.62	3.28	3.72	2.53	–	–	528	0.30
[Ni(sal-1,3-phen)-NaY]	3.38	1.28	0.42	8.12	21.70	8.58	5.29	2.26	2.53	1605	471	394	0.22
Cu(II)-NaY	–	–	–	–	21.48	8.49	3.28	3.86	2.53	–	–	532	0.30
[Cu(sal-1,3-phen)-NaY]	3.35	1.31	0.41	8.23	21.68	8.57	5.27	2.25	2.53	1603	487	390	0.23

[a] Surface area is the "monolayer equivalent area" calculated as explained in the reference 12.
[b] Calculated by the *t*-method (see the text).

and the resulting zeolites were Soxhlet extracted with *N*,*N*-dimethylformamide (for 5 h) and then with ethanol (for 2 h) to remove excess phenylene-1,3-diamine, unreacted [M(sal)$_2$] and any M(II) complexes adsorbed onto the external surface of the zeolite crystallites. The resulting solids were dried at 90 °C under vacuum for 8 h.

2.6. Homogeneous oxidation of cyclohexene

To a solution of cyclohexene (1 ml), [M(sal-1,3-phen)] (1.02×10^{-5} mol) in dichloromethane (10 ml), TBHP (2 ml) was added. The resulting mixture was then refluxed for 8 h under N_2 atmosphere, the solvent evaporated under reduced pressure and the crude analyzed by GC and GCMS. The concentrations of products were determined using cyclohexanone as internal standard.

2.7. Heterogeneous oxidation of cyclohexene

A mixture of 1.0 g catalyst, 25 ml solvent and 10 mmol cyclohexene was stirred under nitrogen atmosphere in a 50 ml round-bottom flask equipped with a condenser and a dropping funnel at room temperature for 30 min. Then 16 mmol of TBHP (solution 80% in di-*tert*-butylperoxide) was added. The resulting mixture was then refluxed for 8 h under N_2 atmosphere. After filtration and washing with solvent, the filtrate was concentrated and then subjected to GC analysis. The concentrations of products were determined using cyclohexanone as internal standard.

3. Results and discussion

Encapsulation of the complexes was performed in the liquid phase by a two-step process that involves: (i) adsorption of a transition metal precursor complex, [M(sal)$_2$]-NaY (M = Mn(II), Co(II), Ni(II), Cu(II)), and (ii) in situ Schiff condensation of the adsorbed metal complex with the phenylene-1,3-diamine; [M(sal-1,3-phen)]-NaY. The resulting materials [M(sal-1,3-phen)]-NaY were purified by Soxhlet extraction with different solvents. In order to characterise the resulting materials and to assess the efficiency of the encapsulation process, the parent zeolite and samples of [M(sal)$_2$]-NaY and [M(sal-1,3-phen)]-NaY, were studied by several techniques and the obtained results compared. Soxhlet extraction was performed only for the zeolites with the complexes [M(sal-1,3-phen)]; the modified zeolites with [M(sal)$_2$] were not purified by extraction as it was observed that this operation leads to a loss of the characteristic colour of the material. This observation provides an indication that [M(sal)$_2$] is free to diffuse out of the zeolite. As these samples were not submitted to Soxhlet extraction, it was expected that they have metal complexes both inside the cavities and adsorbed onto the external surface.

The chemical compositions confirmed the purity and stoichiometry of the neat and nanocavity encapsulated complexes (Tables 1 and 2). The chemical analyses of the samples reveal the presence of organic matter with a C/N ratio roughly similar to that for neat complexes. The mol ratios Si/Al obtained by chemical analysis for zeolites are presented (Table 2).

The Si and Al contents in M(II)NaY and the zeolite complexes; [M(sal-1,3-phen)]-NaY; are almost in the same ratio as in the parent zeolite. This indicates little changes in the zeolite framework due to the absence of dealumination in metal ion exchange. The X-ray diffraction (XRD) patterns of zeolite contained *N*,*N*′-bis(salicylidene)phenylene-1,3-diamine; sal-1,3-phen; complexes are similar to those of M(II)NaY and the parent NaY zeolite. The zeolite crystallinity is retained on encapsulating complexes. Crystalline phase of free metal ions or encapsulation ligand complexes were not detected in any of the patterns as their fine dispersion in zeolite might have rendered them non-detectable by XRD.

The in situ Schiff condensation synthesis, Scheme 1, leads to the encapsulation of manganese(II), cobalt(II), nickel(II) and copper(II) complexes of sal-1,3-phen ligand within the nanodimensional pores of zeolite. The parent NaY zeolite has Si/Al molar ratio of 2.53 which corresponds to a unit cell formula $Na_{56}[(AlO_2)_{56}(SiO_2)_{136}]$ (Table 2). The unit cell formulae of metal-exchanged zeolites show a metal dispersion of around 11 mol per unit cell (Mn(II)NaY, $Na_{33.2}Mn_{11.3}[(AlO_2)_{56}(SiO_2)_{136}]\cdot nH_2O$; Co(II)NaY, $Na_{34}Co_{11}[(AlO_2)_{56}(SiO_2)_{136}]\cdot nH_2O$; Ni(II)NaY, $Na_{33.8}Ni_{11.1}[(AlO_2)_{56}(SiO_2)_{136}]\cdot nH_2O$; Cu(II)NaY, $Na_{34.4}Cu_{10.8}[(AlO_2)_{56}(SiO_2)_{136}]\cdot nH_2O$). The analytical data of each complex indicate M:C:H molar ratios almost close to those calculated for the mononuclear structure. However, the presence of minute traces of free metal ions in the lattice could be assumed as the metal content is slightly higher than the stoichiometric requirement. Only a portion of metal ions in metal-exchanged zeolite has undergone complexation and the rest is expected to be removed on re-exchange with sodium nitrate solution. But, some of these cation sites in the zeolite lattice might be blocked from solution access by the encapsulated complexes. This shielding effect is more probable in the present case since the complex loading level is relatively higher than that reported previously [13]. The traces of free metal ions remaining in zeolite, as has been reported in previous studies [14], are unlikely to cause any serious interference in the behavior of the encapsulated complex.

FTIR data can provide information on the encapsulated metal complexes and on the crystallinity of the host zeolite. The FTIR spectra of NaY and of the modified zeolites are studied. The spectra of NaY and of the modified zeolites are dominated by the strong zeolite bands: a broad band in the range 3700–3300 cm^{-1} due to surface hydroxylic groups and lattice vibrations in the range 1300–450 cm^{-1}. No shift or broadening of these zeolite structure-sensitive vibrations are observed upon inclusion of the complexes, which provides further evidence that the zeolite framework remains unchanged. The bands due to the complexes are weaker (due to a low concentration of the complexes) and thus can only be observed in the regions where the zeolite matrix does not absorb i.e. from 1620–1200 cm^{-1}. The IR bands of $[M(sal)_2]$-NaY occur at frequencies shifted within 2–4 cm^{-1} from those of the free complex $[M(sal)_2]$; furthermore, some changes in band intensities can be observed in the region of the C=O and C=C stretching vibrations (1520–1580 cm^{-1}). These observations not only confirm the presence of $[M(sal)_2]$ in the zeolite, but also suggest that its structure is almost identical to that of the free complex. The IR spectra of [M(sal-1,3-phen)] clearly show the absence of the characteristically coupled $\upsilon(C{=}O) + \upsilon(C{=}C)$ vibration of $[M(sal)_2]$, as expected from the Schiff condensation that took place within the zeolite cavities. The entrapped complexes exhibit very similar IR data that are shifted 4–8 cm^{-1} relative to those of the corresponding free complexes (Table 2). These variations in band frequency can also be attributed to: (i) distortions of the complexes, or to (ii) interactions with the zeolitic matrix (by electrostatic effects or co-ordination—the higher negative charge of the zeolite host makes it a stronger ligand).

Their electronic spectra of Schiff-base in ethanol solutions along with bands assigned to intraligand $\pi \rightarrow \pi^*$ and $n \rightarrow \pi^*$ transitions, also display the absorption maxima at 414–428 nm ($\varepsilon = 310$–$660\ M^{-1}\ cm^{-1}$) attributable to an $n \rightarrow \pi^*$ transition of dipolar zwitterionic keto-amine tautomeric structures of ligand. Electronic spectra of [Cu(sal-1,3-phen)] complexes were recorded in $CHCl_3$ solution over the range 400–700 nm (Table 1). The visible spectra of the [Cu(sal-1,3-phen)] complexes consists of a shoulders at ~490 nm and a maximum or a broad shoulder around 560 nm, which can be assigned to the $dxz,yz \rightarrow dxy$ and $dx^2{-}y^2 \rightarrow dxy$ transitions in D_2h symmetry [15]. The room temperature magnetic moments of [Cu(sal-1,3-phen)] (Table 1) fall in the range 1.74 μB which are typical for square-planar (D_4h) and tetrahedrally distorted (D_2h) mononuclear copper(II) complexes with a $S = 1/2$ spin state and did not indicate any antiferromagnetic coupling of spines at this temperature. The tetrahedral geometry of the [Mn(sal-1,3-phen)] is strongly indicated by similarities in the visible spectra of this chelate with those of known tetrahedral complexes containing oxygen–nitrogen donor atoms [16]. The electronic spectrum of the [Ni(sal-1,3-phen)] exhibit one band at 479 nm which can be assigned to a $d \leftrightarrow d$ transition of the metal ion. The average energy of this absorption is comparable to $d \leftrightarrow d$ transitions of other square-planar Schiff-base of nickel(II) chelates with nitrogen and oxygen donor atoms [17,18], which have reported values in the range of 460–490 nm. The electronic spectrum of [Co(sal-1,3-phen)] is very similar to that reported for [Co(salen)]. The spectrum of the [Co(sal-1,3-phen)] exhibit two bands at 555–660 nm which are assigned to $d \leftrightarrow d$ transitions. In addition, a lower energy absorption at 425 nm has been observed such low energy bands which have recently been shown to be characteristic of square-planar cobalt(II) chelates [16,19]. This geometry is confirmed by the values of the effective magnetic moment (Table 1).

The nitrogen adsorption isotherms for the parent and the modified zeolites are typical of microporous solids; however, a decrease in the adsorption capacity of the zeolite was observed after adsorption of $[M(sal)_2]$, and a further decrease after Schiff base condensation. The micropore volume and surface area are presented in Table 2. The large reduction in surface area and in micropore volume observed for the M-based zeolites is interpreted as arising from the presence of compounds in the zeolite cavities. The values of the micropore volume and surface area of [M(sal-1,3-phen)]-NaY are similar to those observed in NaY zeolites with entrapped macrocyclic polyaza and Schiff-base

complexes [20,21]. As the metal content in all samples is of the same magnitude, the observed lowering of the micropore volume on going from [M(sal)$_2$] to [M(sal-1,3-phen)] must be attributed to the large volume of the latter complexes thus providing an additional confirmation that Schiff condensation took place within the zeolite nanocavities.

The X-ray powder diffractograms (XRD) of NaY, Ni(II)NaY and HGNM were recorded to study their crystallinity and to ensure encapsulation. After careful comparison of XRD patterns of NaY and Ni(II)NaY, it was observed that, there was one new peak with a *d* value of 1.740 nm in Ni(II)NaY. This peak was also observed in HGNM and neat complexes at the same position. In addition, the HGNM exhibits one new signal with value of 8.420 nm, which is a part of the ligand as this signal was also observed in neat complexes but not observed in NaY or Ni(II)NaY. This information clearly indicated the support of [Ni(sal-1,3-phen] in the nanodimensional pores of zeolite-Y. Very low intensity of other peaks made it difficult to distinguish them from the other peaks in the XRD pattern of the encapsulated zeolite. This indicated that the crystallinity and morphology of zeolite were preserved during encapsulation.

The oxidation of cyclohexene is negligible in the absence of transition metal catalysts confirming that under the conditions of the experiments, the oxidation is indeed catalytic in nature. In the case of the encapsulated catalysts, metal was not detected in the reaction products by AAS indicating that oxidation of cyclohexene by dissolved metal complexes leached out from the zeolite matrix is negligible. The zeolites alone without the metal complexes were also catalytically inactive. Since the concentration of uncomplexed metal ions in the catalysts is also negligible, their contribution to catalytic activity may be neglected. Further evidence to confirm that the oxidation of cyclohexene is indeed catalyzed to a significant extent by the solid zeolite catalyst containing the encapsulated metal complex and not by the free complex dissolved in solution was obtained as follows. In one set of two identical experiments, the solid catalyst ([Mn(Sal-1,3-phen)]-NaY) was removed by centrifugation after a reaction time of 8 h. While the conversion of cyclohexene proceeded further in the presence of the solid catalyst, there was no further conversion of cyclohexene when the catalyst was removed from the reaction system. The following points may be noted:

1. The major products of oxidation of cyclohexene are 2-cyclohexene-1-one and 2-cyclohexene-1-ol.
2. The zeolite-encapsulated complexes did not undergo any colour change during the reaction and could be easily separated and reused many times. In contrast, the neat complexes, while they were active in the first cycle, were completely destroyed during the first run and changed colour.
3. The neat complexes gave low conversions compared to the encapsulated catalysts. This may be a consequence of (2) above, since, due to the continuous degradation of the catalyst, the effective concentration of the catalyst will be lower than that taken initially.
4. The sal-1,3-phen ligand alone in the absence of metal were not catalytically active.

Table 3
Oxidation of cyclohexene with TBHP catalyzed by metal complexes in CH_2Cl_2

Catalyst	Conversion (%)	Selectivity (%)		
		Ketone[a]	Alcohol[b]	Peroxide[c]
[Mn(sal-1,3-phen)]	54.3	60.3	26.4	13.3
[Mn(sal-1,3-phen)][d]	35.7	52.8	28.5	18.7
[Mn(sal-1,3-phen)][e]	48.6	62.6	27.2	10.2
[Mn(sal-1,3-phen)][f]	20.9	64.5	27.1	8.4
[Co(sal-1,3-phen)]	43.6	50.2	36.7	13.1
[Ni(sal-1,3-phen)]	22.4	38.5	43.4	18.1
[Cu(sal-1,3-phen)]	35.6	41.2	35.5	23.3

[a] 2-Cyclohexene-1-one.
[b] 2-Cyclohexene-1-ol.
[c] 1-(*tert*-Butylperoxy)-2-cyclohexene.
[d] Catalyst = 0.5×10^{-5} mol.
[e] Catalyst = 2.04×10^{-5} mol.
[f] Catalyst = 4.08×10^{-5} mol.

5. The activity of cyclohexene oxidation decreases in the series [Mn(sal-1,3-phen)]-NaY > [Co(sal-1,3-phen)]-NaY > [Cu(sal-1,3-phen)]-NaY > [Ni(sal-1,3-phen)]-NaY.
6. At the end of reaction, the catalyst was separated by filtrations, thoroughly washed with solvent and reused under similar conditions by AAS which showed no reduction in the amount of metal.
7. The trend observed in Tables 3 and 4 can be explained by the donor ability of ligand available in the complex catalysts. As Wang and co-workers have pointed out recently, the key point in the conversion of cyclohexene to the products is the

Table 4
Oxidation of cyclohexene with TBHP catalyzed by nanodimensional pores of zeolite-Y-encapsulated metal complexes in CH_2Cl_2

Catalyst	Conversion (%)	Selectivity (%)		
		Ketone[a]	Alcohol[b]	Peroxide[c]
[Mn(sal-1,3-phen)]-NaY	84.6	84.2	14.7	1.1
[Mn(sal-1,3-phen)]-NaY[d]	83.9	83.8	14.9	1.3
[Mn(sal-1,3-phen)]-NaY[e]	83.4	83.1	15.2	1.7
[Mn(sal-1,3-phen)]-NaY[f]	82.9	82.4	15.0	2.6
[Mn(sal-1,3-phen)]-NaY[g]	76.5	73.8	20.7	5.5
[Mn(sal-1,3-phen)]-NaY[h]	84.8	84.5	14.3	1.2
[Mn(sal-1,3-phen)]-NaY[i]	85.1	86.3	12.8	0.9
[Mn(sal-1,3-phen)]-NaY[k]	82.4	83.5	14.6	1.9
[Mn(sal-1,3-phen)]-NaY[l]	68.5	69.7	20.7	9.6
[Mn(sal-1,3-phen)]-NaY[m]	60.2	59.1	32.4	8.5
[Co(sal-1,3-phen)]-NaY	57.2	70.2	21.3	8.5
[Ni(sal-1,3-phen)]-NaY	30.3	57.5	30.2	12.3
[Cu(sal-1,3-phen)]-NaY	41.4	58.9	24.7	16.4

[a] 2-Cyclohexene-1-one.
[b] 2-Cyclohexene-1-ol.
[c] 1-(*tert*-Butylperoxy)-2-cyclohexene.
[d] First reuse.
[e] Second reuse.
[f] Third reuse.
[g] Catalyst = 0.50 g.
[h] Catalyst = 1.50 g.
[i] Catalyst = 2.0 g.
[k] Solvent = chloroform.
[l] Solvent = methanol.
[m] Solvent = acetonitrile.

reduction of L-Mn^{3+} to L-Mn^{2+}. This reduction to L-Mn^{2+} is facilitated with the ligands available around the metal cation [23].

8. The formation of the allylic oxidation products 2-cyclohexene-1-one and 2-clohexene-1-ol shows the preferential attack of the activated C–H bond over the C=C bond. The formation of 1-(*tert*-butylperoxy)-2-cyclohexene shows the presence of radical reactions [24]. TBHP as oxidant promotes the allylic oxidation pathway and epoxidation is minimized, especially under the acidic properties of zeolite encapsulated with divalent and trivalent transition metal ions and complexes, has been observed by us and others [25].
9. The effect of various solvents for the oxidation of cyclohexene with [Mn(sal-1,3-phen]-NaY catalysts was also studied (Table 4). In all the oxidation reaction, 2-cyclohexene-1-one was formed as the major product. When the reaction was carried out in a coordinating solvent like CH_3CN the conversion decreased by a factor of ∼1.56. This might be attributed to donor number of acetonitrile (14.1) and therefore, its higher ability to occupy the vacant spaces around the metal center and prevent the approaching of oxidant molecules. In dichloromethane and chloroform the yields of 2-cyclohexene-1-o1 and 2-cyclohexene-1-one were higher and lower yield of the peroxy species was obtained as compared to the other solvents. The efficiency of the catalysts for cyclohexene oxidation in different solvents decreases in the order: dichloromethane > chloroform > methanol > acetonitrile.
10. The effect of transition metal complexes encapsulated in zeolite; [M(sal-1,3-phen)]-NaY; was studied on the oxidation of cyclohexene with TBHP in dichloromethane and the results are shown in Table 4. As shown in Table 4, only allylic oxidation has occurred with the formation of 2-cyclohexene-1-one, 2-cyclohexene-1-ol and 1-(*tert*-butylperoxy)-2-cyclohexene. Oxidation with the same oxidant in the presence of Mn(II)NaY was 51.4% [22]. The increase of conversion from 51.4% [22] to 84.6% compared to Mn(II)NaY with [Mn(sal-1,3-phen)]-NaY indicates that the existence of ligand has increased the activity of the catalyst by a factor of 1.65. From the indicated results in Tables 3 and 4 it is evident that 2-cyclohexene-1-one is selectively formed in the presence of all catalysts.

One-electron oxidants: Co(II), Mn(II), Cu(II) and Ni(II) catalyze free radical autoxidation processes by promoting the decomposition of TBHP into chain initiating alkoxy and alkyl peroxy radicals in one-electron transfer processes (reactions (1) and (2)). Strictly speaking the metal ion acts as an initiator of free radical autoxidation, which proceeds further via reactions (3)–(6), rather than a catalyst.

$$ROOH + M^{2+} \rightarrow M^{3+}\text{-}OH + RO^{\bullet} \quad (1)$$

$$M^{3+}\text{-}OH + ROOH \rightarrow M^{2+} + ROO^{\bullet} + H_2O \quad (2)$$

$$RO^{\bullet} + R'H \rightarrow ROH + R'^{\bullet} \quad (3)$$

$$R'^{\bullet} + ROO^{\bullet} \rightarrow ROOR'^{\bullet} \quad (4)$$

$$R'^{\bullet} + M^{3+}\text{-}OH \rightarrow M^{2+} + R'\text{-}OH \quad (5)$$

$$M^{3+}\text{-}OH + R'\text{-}OH \rightarrow H_2O + R'{=}O \quad (6)$$

Metal ions which catalyze oxygen transfer reactions with TBHP can be divided into two types based on the active intermediate: a peroxometal or an oxometal complex [26]. Peroxometal pathways usually involve early transition elements with d^0 configuration, e.g. Mo(VI), W(VI), V(V) and Ti(IV). Late or first row transition elements, e.g. Cr(VI), V(V), Mn(V), Ru(VI), Ru(VIII) and Os(VIII), generally employ oxometal pathways. Some elements, e.g. vanadium, can employ oxometal or peroxometal pathways depending on the substrate. Reactions that typically involve peroxometal pathways are olefin epoxidation and heteroatom oxidations. Oxometal species, on the other hand, display a broader range of activities, including allylic oxidations. An important difference is that peroxometal pathways do not involve any change in oxidation state of the metal, i.e. the metal acts as a Lewis acid and activity is not restricted to variable valence elements. An oxometal pathway, in contrast, involves two-electron redox reactions of the metal ion. Furthermore, it should be emphasized that most metals, which catalyze oxygen transfer processes, via peroxometal or oxometal pathways, are also capable of catalyzing one-electron transfer processes with peroxides. Consequently, competition from free radical processes is often observed, to a greater or lesser extent, in oxygen transfer processes. When TBHP are used as oxidants hemolytic versus heterolytic processes can be distinguished by the use of suitable probe molecules [27,28]. We also note that immobilization of a redox-active element in a solid matrix will probably not influence the oxidation mechanism, e.g. one-electron oxidants will still catalyze free radical processes when incorporated in the framework of a molecular sieve.

Table 5 shows the ship-in-a-bottle catalysts, oxidants and substrates that have been reported. Much of the early work in this area involved the oxygen atom transfer agent iodosylbenzene (PhIO) as the oxidant. Unfortunately, the activity of PhIO/zeolite systems generally decays rapidly because of pore blockage by iodoxybenzene [29]. MnPc/NaY was shown to oxidize various olefins to the corresponding epoxides, however, the activity was lower than the for the free MnPc complex [30]. Similarly, CoPc encapsulated in NaY was more active than the free complex with time but to be fair the homogeneous CoPc catalyst decomposes during this period [31]. [Mn(salen)]@NaY has also been shown to be an epoxidation catalyst, however, the selectivity was not as high and diffusional problems were noted [32]. All of these results suggest that iodosylbenzene is a poor choice of oxidant and that diffusion in and out of the zeolite may be the limiting factor. Dioxygen would be the ideal source of oxygen both from an economic and byproduct point of view. Unfortunately, O_2 is much more difficult to activate compared with reduced forms of oxygen such as peroxides [33,34]. The results clearly suggest that [Mn(sal-1,3-phen)]@NaY efficiently catalyzes conversion of cyclohexene to 2-cyclohexene-1-one with 84.2% selectivity. The more activity of sal-1,3-phen system has clearly arisen from the existence of electron donating ligand which facilitate the

Table 5
Oxidation of cyclohexene catalyzed by zeolite encapsulated transition metal complexes

Catalyst	Oxidant	Comments	Ref.
[Mn(salen)]@NaY	PhIO	Major product is epoxide	[32]
[Co(Pc)]@NaY	PhIO	Major product is epoxide	[30]
[FePc]@NaY	TBHP	High activity, deactivates	[35]
[FePc]/NaY/PDMS[a]	TBHP	Highest activity so far	[36]
FePc/VPI-5	TBHP	Less active than zeolites	[37]
[$RuF_{16}Pc$]@NaX	TBHP	Major product is cyclohexanone, high activity	[38]
[$Mn(bipy)_3$]@NaY	H_2O_2	Adipic acid 1,2-dione, 1,2-diol	[39]
[VO(salen]@NaY	TBHP	Epoxidation of cyclohexene	[40]
[Mn(NNNN)]$^{2+}$@NaY[b]	TBHP	major product is di 2-cyclohexenyl ether	[22]
[Ni(salen)]@NaY	NaOCl	Major product is epoxide	[41]
[Ni(salen)]@NaY	$KHSO_3$	Major product is epoxide	[41]
[Mn(salen)]$^{+}$@NaY	NaOCl	Major product is epoxide	[41]
[Mn(salen)]$^{+}$@NaY	$KHSO_3$	Major product is epoxide	[41]
[Mn(salen)]$^{+}$@Clay	$KHSO_3$	Major product is epoxide	[41]
[Ni(R_2Bzo_2[14]aneN_6)]$^{2+}$@NaY[c]	O_2	Major product is 2-cyclohexene-1-ol	[42]
[Ni(Me_6[14]ane N_4)]$^{2+}$@NaY[d]	O_2	Major product is 2-cyclohexene-1-ol	[43]
[Mn(sal-1,3-phen)]@NaY	TBHP	major product is 2-cyclohexene-1-one	This work

[a] PDMS = Polydimethylsiloxane membrane.
[b] NNNN = Ethylenediamine, tetramethylethylenediamine, 2,2 –bipyridine or tetramethyl-1,8-naphthalenediamine.
[c] (R_2Bzo_2[14]aneN_6): 3,10-dialkyl-dibenzo-1,3,5,8,10,12-hexaazacyclotetradecane.
[d] (Me_6[14]aneN_4): 5,7,7,12,14,14-hexamethyl-1,4,8,11-tetraazacyclotetradecane-4,11-diene.

electron transfer rate, a process that has previously observed by us in other oxidation reactions [5–10,25,32–42]. All conversions efficiency with high selectivity obtained in this study is significantly higher than that obtained using metal containing porous and non-porous materials [25,32–42].

Acknowledgment

Authors are grateful to Council of University of Kashan for providing financial support to undertake this work.

References

[1] D.E. DeVos, F. Thibault-Starzyk, P.P. Knops-Gerrits, R.F. Parton, P.A. Jacobs, Macromol. Symp. 80 (1984) 157.
[2] K.J. Balkus Jr., A.K. Khanmamedova, K.M. Dixon, F. Bedioui, Appl. Catal. A: Gen. 143 (1996) 159.
[3] D.E. DeVos, P.P. Knops-Gerrits, R.F. Parton, B.M. Weckhuysen, P.A. Jacobs, R.A. Schoonheydt, J. Inclusion Phenom. Mol. Recognit. Chem. 21 (1995) 185.
[4] F. Bedioui, Coord. Chem. Rev. 144 (1995) 39;
J. Połtowicz, K. Pamin, E. Tabor, J. Haber, A. Adamski, Z. Sojka, Appl. Catal. A: Gen. 299 (2006) 235;
J. Haber, K. Pamin, J. Połtowicz, J. Mol. Catal. A: Chem. 224 (2004) 153;
S. Deshpande, D. Srinivas, P. Ratnasamy, J. Catal. 188 (1999) 261;
S.P. Varkey, C. Ratnasamy, P. Ratnasamy, J. Mol. Catal. A: Chem. 135 (1998) 295;
C.R. Jacob, S.P. Varkey, P. Ratnasamy, Appl. Catal. A: Gen. 168 (1998) 353;
E. Briot, F. Bedioui, K.J. Balkus Jr., J. Electron. Chem. 454 (1998) 83.
[5] B. Romanovsky, Macromol. Symp. 80 (1994) 185.
[6] M. Salavati-Niasari, J. Mol. Catal. A: Chem. 217 (2004) 87.
[7] M. Salavati-Niasari, Inorg. Chem. Commun. 7 (2004) 963.
[8] M. Salavati-Niasari, M. Bazarganipour, Catal. Commun. 8 (2006) 336.
[9] M. Salavati-Niasari, H. Najafian, J. Chem. Res. 9 (2003) 536.
[10] M. Salavati-Niasari, J. Mol. Catal. A: Chem. 245 (2006) 192.
[11] M.N. Patel, N.H. Patel, K.N. Patel, P.P. Dholakiya, D.H. Patel, Synth. React. Inorg., Metal-Org. Nano-Met. Chem. 33 (2003) 51;
M.N. Patel, N.H. Patel, P.K. Panchal, D.H. Patel, Synth. React. Inorg., Metal-Org. Nano-Met. Chem. 34 (2004) 873.
[12] S.W. Wang, H. Everett, R.A.W. Haul, L. Moscou, R.A. Pierotti, J. Rouquerol, T. Siemieniewska, Pure Appl. Chem. 57 (1985) 603;
A. Lineares-Solano, Textural characterization of porous carbons by physical adsorption of gases, in: J.L. Figueiredo, J.A. Moulijn (Eds.), Carbon and Coal Gasification, M. Nijhoff, M.A. Dordrecht, 1986, p. 137.
[13] N. Herron, G.D. Stucky, C.A. Tolman, J. Chem. Soc. Chem. Commun. (1986) 1521.
[14] H. Diegruber, P.J. Plath, G. Schulz-Ekloff, M. Mohl, J. Mol. Catal. 24 (1984) 115.
[15] A.H. Maki, B.R. McGarvey, J. Chem. Phys. 29 (1958) 35;
I. Bertini, G. Canti, R. Grassi, A. Scozzafava, Inorg. Chem. 19 (1980) 2198.
[16] N. Raman, Y.P. Raja, A. Kulandaisamy, Proc. Indian Acad. Sci. (Chem. Sci.) 113 (2001) 183.
[17] A.B. Lever, Inorganic Electronic Spectroscopy, second ed., Elsevier, New York, 1968.
[18] R.H. Holm, G.W. Evverett, A. Chakrvorty, Prog. Inorg. Chem. 7 (1966) 183.
[19] C.A. Root, B.A. Rising, M.C. Vanderveer, C.F. Hellmuth, Inorg. Chem. 11 (1972) 1489;
F.L. Urbach, R.D. Bereman, J.A. Topido, M. Hariharan, B.J. Kalbacher, J. Am. Chem. Soc. 92 (1970) 792;
M.A. Hitchman, Inorg. Chem. 16 (1977) 1985.
[20] M. Salavati-Niasari, Microporous Mesoporous Mater. 92 (2006) 173;
M. Salavati-Niasari, Inorg. Chem. Commun. 9 (2006) 268;
M. Salavati-Niasari, F. Davar, Inorg. Chem. Commun. 9 (2006) 304;
M. Salavati-Niasari, M. Bazarganipour, Inorg. Chem. Commun. 9 (2006) 332;
M. Salavati-Niasari, A. Amiri, Trans. Met. Chem. 31 (2006) 157;
M. Salavati-Niasari, A. Amiri, Trans. Met. Chem. 30 (2005) 720.
[21] K.J. Balkus, A.G. Gabrielov, J. Inclu, Phenom. Mol. Recognit. Chem. 21 (1995) 159.
[22] M.S. Niassary, F. Farzaneh, M. Ghandi, L. Turkian, J. Mol. Catal. A: Chem. 157 (2000) 183.
[23] M. Wang, C.J. Hao, Y.P. Wang, S.B. Li, J. Mol. Catal. A: Chem. 147 (1999) 173.
[24] D. Koola, J.K. Kochi, J. Org. Chem. (1987) 4545.
[25] A.H. Gemeay, M.A. Salem, I.A. Salem, Colloid Surf. 117 (1996) 245;
M. Salavati-Niasari, F. Farzaneh, M. Ghandi, J. Mol. Catal. A: Chem. 186 (2002) 101;

M. Salavati-Niasari, H. Banitaba, J. Mol. Catal. A: Chem. 201 (2003) 43;
M. Salavati-Niasari, J. Hasanalian, H. Najafian, J. Mol. Catal. A: Chem. 209 (2004) 204;
M. Salavati-Niasari, A. Amiri, Appl. Catal. A: Gen. 290 (2005) 46;
M. Salavati-Niasari, M.R. Elzami, M.R. Mansournia, S. Hydarzadeh, J. Mol. Catal. A: 221 (2004) 169;
M. Salavati-Niasari, P. Salemi, F. Davar, J. Mol. Catal. A: Chem. 238 (2005) 215;
M. Salavati-Niasari, T. Khosousi, S. Hydarzadeh, J. Mol. Catal. A: Chem. 235 (2005) 150;
M. Salavati-Niasari, S. Hydarzadeh, J. Mol. Catal. A: Chem. 237 (2005) 254.

[26] R.A. Sheldon, Top. Curr. Chem. 164 (1993) 21.
[27] P.A. MacFaul, I.W.C.E. Arends, K.U. Ingold, D.D.M. Wayner, J. Chem. Soc. Perkin Trans. 2 (1997) 135.
[28] I.W.C.E. Arends, K.U. Ingold, D.D.M. Wayner, J. Am. Chem. Soc. 117 (1995) 4710.
[29] C.R. Jacob, S.P. Varkey, P. Ratnasamy, Appl. Catal. A: Gen. 182 (1999) 91.
[30] E. Paez-Mozo, N. Gabriunas, R. Maggi, D. Acosta, P. Ruiz, B. Delmon, J. Mol. Catal. 91 (1994) 251.
[31] Z. Jiang, Z. Xi, J. Mol. Catal. (Chin.) 6 (1992) 467.
[32] C. Bowers, P.K. Dutta, J. Catal. 122 (1990) 271.
[33] A. Zsigmond, F. Notbeisz, M. Bartok, J.E. Backvall, Stud. Surf. Sci. Catal. 78 (1993) 417.
[34] A. Zsigmond, F. Notheisz, Zs. Szegletes, J.E. Backvall, Stud. Surf. Sci. Catal. 94 (1995) 728.
[35] R.F. Parton, C.P. Bezouhanova, J. Grobet, P.J. Grobet, P.A. Jacobs, Stud. Surf. Sci. Catal. 83 (1994) 371.
[36] R.F. Patton, I.F.J. Vankelecom, M.J.A. Casselman, C.P. Bezouhanova, J.B. Uytterhoeven, P.A. Jacobs, Nature 370 (1994) 541.
[37] R.F. Parton, C.P. Bezouhanova, F. Thibault-Starzyk, R.A. Reynders, P.J. Grobet, P.A. Jacobs, Stud. Surf. Sci. Catal. 84 (1994) 813.
[38] K.J. Balkus Jr., M. Eissa, R. Lavado, Stud. Surf. Sci. Catal. 94 (1995) 713; K.J. Balkus Jr., M. Eissa, R. Lavado, J. Am. Chem. Soc. 117 (1995) 10753.
[39] P.P. Knops-Gerrits, F. Thibault-Starzyk, P.A. Jacobs, Stud. Surf. Sci. Catal. 84 (1994) 1411.
[40] K.J. Balkus Jr., A.K. Khanrnamedova, K.M. Dixon, F. Bedioui, Appl. Catal. A: Gen. 143 (1996) 159.
[41] D. Chatterjee, A. Mitr, J. Mol. Catal. A: Chem. 144 (1999) 363.
[42] M. Salavati-Niasari, F. Davar, Inorg. Chem. Commun. 9 (2006) 263.
[43] M. Salavati-Niasari, J. Mol. Catal. A: Chem. 229 (2005) 159.